Spiky gold shells on magnetic particles for DNA biosensors

Erin Bedford, Souhir Boujday, Claire-Marie Pradier, Frank Gu

Spiky gold shells on magnetic particles for DNA Biosensors

Erin E. Bedford[1,2] , Souhir Boujday[1*], Claire-Marie Pradier[1], and Frank X. Gu[2*]

[1] Sorbonne Universités, UPMC Univ Paris 06, CNRS, Laboratoire de Réactivité de Surface (LRS), UMR 7197, 4 Place Jussieu, Case 178, F-75252, Paris, France
[2]Department of Chemical Engineering, and Waterloo Institute for Nanotechnology, University of Waterloo, 200 University Ave. W., Waterloo, ON, N2L 3G1, Canada

*Corresponding authors. Contacts: souhir.boujday@upmc.fr, +33 1 44 27 60 01 or frank.gu@uwaterloo.ca, +1 519 888 4567 ext.38605.

Table (1)
Figures (8)
Words (4411)

Abstract

Combined separation and detection of biomolecules has the potential to speed up and improve the sensitivity of disease detection, environmental testing, and biomolecular analysis. In this work, we synthesized magnetic particles coated with spiky nanostructured gold shells and used them to magnetically separate out and detect oligonucleotides using SERS. The distance dependence of the SERS signal was then harnessed to detect DNA hybridization using a Raman label bound to a hairpin probe. The distance of the Raman label from the surface increased upon complementary DNA hybridization, leading to a decrease in signal intensity. This work demonstrates the use of the particles for combined separation and detection of oligonucleotides without the use of an extrinsic tag or secondary hybridization step.

Keywords: Magnetic particles; Plasmonic; nanostructured gold; SERS; DNA biosensor

Introduction

Nanotechnology has led to faster, more sensitive, and more selective methods of biomolecule detection.[1,2] In addition, it has offered the possibility of miniaturization and the ability to combine the steps required for detection into a single platform. By combining multiple steps (concentration, purification, detection) into a single platform, we can envisage new applications in point-of-care diagnostics, environmental testing, and biomolecular analysis.

Magnetic particles are commonly used for separating and concentrating specific biomolecules.[3-7] The benefits of magnetic particles for biomolecule concentration and separation include a simple and inexpensive set-up (typically requiring only the particles themselves and a magnet), no extensive technical training, and result in

highly sensitive and selective separation.[8] Superparamagnetic particles are considered optimal since they will remain dispersed when added to a sample, allowing the analyte to bind to their surface, but will be separated when a magnet is used.[9,10] A challenge with using superparamagnetic particles is that separation times are often prohibitively long.[11,12] One method that has been used to overcome this is to use controlled aggregates (150-300 nm) of superparamagnetic nanoparticles (~20 nm) to increases the total magnetic moment while still maintaining the superparamagnetic properties of the particles.

In most cases where magnetic particles are used, the purified biomolecule is dissociated from the magnetic particles for subsequent analysis. Since the biomolecule is already pre-concentrated and specifically bound to the surface, an interesting possibility is to directly detect it while still attached using a surface-sensitive detection method. Surface-enhanced Raman spectroscopy (SERS) relies on the electromagnetic enhancement induced by nanostructured metal surfaces (typically gold or silver) to greatly increase the Raman signal (enhancements on the order of 10^4-10^7).[13] SERS also offers fingerprint specificity, which leads to the possibilities of highly specific detection and multiplexing. Coating magnetic particles with a nanostructured metal can therefore enable combined magnetic separation and SERS detection of molecules bound to the particle surface.

Several other researchers have investigated forming nanostructured gold shells on various core particles.[14] Gold nanostars with small iron oxide cores (gold nanostars: ~100 nm, iron oxide cores: <30 nm) have been synthesized for use in gyromagnetic imaging,[15,16] as recyclable catalysts,[17] for protein separation and SERS detection,[18] and for enhanced electromagnetic properties.[19,20] Others have formed nanostructured gold shells on cores of various materials including polymer beads,[21,22] block copolymer assemblies,[21] gold nanowires,[23] gold nanorods,[24], and other metallic particles.[25-27]

Label-free methods of detection using SERS are of interest because they can reduce the number of steps required for detection and because of the fingerprint specificity obtainable by SERS. Label-free detection of nucleic acids using SERS has been used to quantitatively analyze ssDNA,[28] identify single-base mismatches,[29,30] and to differentiate between ssDNA and dsDNA,[31-33]. This latter task can still be challenging, especially at the low concentrations seen with hybridization detection, since the same four bases are usually present in both probe and target. In addition, when this involves selective capture, a capture probe must first be bound to the surface, leading to an orientation-dependent signal[31,34] that can increase the challenge of hybridization detection.

Another approach is to harness the distance dependence of the signal by using a Raman tag bound to the probe; the probe is designed so that the proximity of the tag relative to the surface changes upon target binding, resulting in a signal change.[35-40] While this approach loses the direct correlation between the molecule and the signal (and thus potential information on the nature of the binding interaction), it still has the benefit of not requiring an extrinsic tag and has the potential for quantitative measurement of binding, both being beneficial features in a DNA detection method. It also offers the potential for multiplexed detection, as different tags providing different Raman signals can easily be used.[41,42]

In this work, we synthesized magnetic particles coated with a nanostructured gold shell that acts as a SERS substrate. To show the effectiveness of the particles in biosensing, we used them to detect oligonucleotide hybridization. This is, to our knowledge, a first example of combined magnetic separation and SERS detection of oligonucleotides without the use of an extrinsic tag.

Material and Methods

Materials

Gold(III) chloride hydrate ($HAuCl_4 \cdot xH_2O$), cetyl trimethylammonium bromide (CTAB), sodium borohydride ($NaBH_4$), silver nitrate ($AgNO_3$), and ascorbic acid, were purchased from Sigma Aldrich. Millipore water and reagent grade ethanol were used. Silica-coated iron oxide particles were synthesized previously at the University of Waterloo [43].

All oligonucleotides were purchased from IDT (Integrated DNA Technologies, Coralville, Iowa). DNA stock solutions were prepared in Millipore water then diluted in buffer purchased as a disulphide and reduced to a thiol using tris(2-carboxyethyl)phosphine (TCEP), purchased from Sigma Aldrich. For the oligonucleotide ruler experiment, the sequences used are listed in Table 1. For the experiment investigating the signal differences between ssDNA and dsDNA, the sequence of the untagged, non-hairpin probe was –S-$(CH_3)_6$-5'-GIGGTTGGTTGTGTTGGGTGTTGTGTCCAACCCC-3', the complementary target sequence was 5'-ACACAACACCCAACACAACCAACCCC-3', and the non-complementary target sequence was 5'-ACACACACACACACACACACACACCC-3'. The sequence of the tagged hairpin probe, also used for the hybridization experiments, was Cy5-5'-TTTTTCGCTCCCTGGTGCCGTAGATGAGCGTTTTT-3'-$(CH_3)_3$-S- (purchased as a disulphide), the complementary target sequence was 5'-ATCTACGGCACCAGG-3', and the non-complementary target sequence was 5'-TCACACGGAGGCTAC-3'. Both 3-mercapto-1-propanol (MCP) and 6-mercapto-1-hexanol (MCH) were purchased from Sigma Aldrich.

Particle synthesis

Particle synthesis was done in several steps: magnetite sphere synthesis, silica coating and functionalization, gold seed binding, then growth of the gold seeds into spikes (Figure 1).

Figure 1: Schematic diagram of spiky particle synthesis steps. Gold seeds are bound to a silica-coated magnetite particle, then grown into gold spikes using a gold salt and CTAB bath solution.

Synthesis of magnetite spheres

Magnetite spheres were synthesized using a previously developed hydrothermal synthesis [43-45]. In brief, sodium citrate dihydrate, polyacrylamide (PAM), and $FeCl_3 \cdot 6H_2O$ were mixed and dissolved in Millipore water. A small amount of ammonium hydroxide was then added to the solution under vigorous stirring. This mixture was poured into a 125 mL PTFE-lined stainless steel pressure vessel (Parr Instrument Company) and heated at 200°C for 12 h. The product was recovered magnetically and washed with deionized water and ethanol by magnetic decantation, then dried under nitrogen.

Magnetic separation of samples in all steps was performed using either a small neodymium magnet or a rare earth homogenous magnetic separator (Sepmag Lab 2142, inner bore diameter 31 mm, radial magnetic field gradient 45 T/m). The samples were placed in or near the magnet and left to separate for 1-2 minutes. The supernatant was then gently removed using a pipette.

Silica coating and functionalization

Silica coating was done in a second step[43]. In brief, the magnetite particle powder was dispersed into a solution of EtOH and Millipore deionized water by probe sonication. Ammonium hydroxide was then added to the dispersion, followed by the slow dropwise addition of TEOS in EtOH solution over 1 h under vigorous mechanical stirring. This mixture was then stirred at room temperature for 18 h, after which the product was recovered magnetically and washed with EtOH by magnetic decantation, then dried under nitrogen.

Silica-coated magnetite particles were functionalized with thiol groups by first functionalizing the surface with amine groups using (3-aminopropyl)triethoxysilane (APTES), then by linking 11-mercaptoundecanoic acid (MUA) to these groups. The particles were dispersed in 2:1 ethanol:Millipore water for a final concentration of 5 mg/mL by bath sonication. While mechanically stirring the particles in a 50°C water bath, 20% v/v APTES solution was quickly added so that the final APTES concentration was 2% v/v. After 24 hours of stirring at 50°C, the particles in solution were magnetically separated and decanted, washed, and dried. To bind the MUA to the amine groups, the carboxylic acid groups were activated by adding 12 mM of NHS and 12 mM of EDC to 10 mM MUA in ethanol and left for 15 minutes. The particles were dispersed in the activated MUA solution and mechanically mixed for 90 minutes. The particles were then magnetically decanted and washed three times in ethanol by magnetic separation.

Gold seed binding

Gold seeds were prepared by warming 5 mL of 0.2 M CTAB in Millipore water to 30°C using a water bath, then by adding 0.125 mL of 0.01 M $HAuCl_4 \cdot xH_2O$ to the vial while magnetically stirring. The bright yellowish-orange solution was stirred for 5 minutes. While still under magnetic stirring in the water bath, 0.06 mL of 0.05 M $NaBH_4$ in Millipore water was added. The light brown solution was stirred for 10 minutes.

Silica-coated magnetite spheres were dispersed in ethanol at 2 mg/mL using a sonic bath. These were combined with equal parts Millipore water and gold seeds (1 mL of each) and mixed by gentle shaking. The mixture was placed on a gentle rotating mixer for 1 hour. The particles were then magnetically decanted, washed three times using magnetic separation in 1 mM CTAB in water, and redispersed in the same volume of 1 mM CTAB as the ethanol that was first used to disperse particles at 2 mg/mL.

Gold shell growth

Growth solution (20 mL) was prepared by adding 1 mL of 0.01 M $HAuCl_4 \cdot xH_2O$ and 0.2 mL of 0.01 M $AgNO_3$ to 100 mM CTAB, then partially reducing the metal salts using 0.16 mL of 0.1 M ascorbic acid (final concentration of 0.5 mM $HAuCl_4$, 0.1 mM $AgNO_3$, and 0.8 mM ascorbic acid). The solution was warmed to 30°C using a water bath and magnetically stirred for 10 minutes. Following this, 400 µL seeded particles were added to 20 mL of growth solution and gently mixed. The mixture was kept at 30°C using for 30 minutes. During growth, the initially light brown solution turned dark grey. The particles in the bath were magnetically decanted, washed three times using magnetic separation in 10 mM CTAB, and stored in 400 µL of 10 mM CTAB.

Particle characterization

Transmission electron microscopy (TEM, Philips CM10) was used to characterize the size and shape of the particles. Samples for all methods were prepared by diluting 25 µL of particles at the final listed concentrations with 1 mL of Millipore water. Magnetization curves were acquired by a superconducting quantum interference device (SQUID) magnetometer at 300K using particles dried in air.

Oligonucleotide binding and detection

Oligonucleotide ruler binding

Disulfide-modified oligonucleotides were diluted to 100 µM and mixed with an equal volume of acetate buffer (500 mM, pH 5.2). To reduce the disulfides into thiol groups, TCEP was prepared at 10 mM and added at 5 µL for every 100 µL of above solution; this was left at room temperature for 1 hour. For each sample, 50 µL of gold-coated magnetic particles were used. The particles in CTAB solution were magnetically decanted; then 100 µL of Millipore water with 0.1% Tween 20 and 52.5 µL of the above oligonucleotide solution were added for each of the different oligonucleotides.

ssDNA and dsDNA binding

Disulfide-functionalized probe oligonucleotides (100 µM) were combined with an equal concentration of complementary oligonucleotides or non-complementary oligonucleotides, or an equivalent volume of water (for ssDNA samples) and diluted to 25 µM in 100 mM acetate buffer with 0.04% Tween 20. To reduce the disulfides into thiol groups, TCEP was prepared at 10 mM and added at 20 µL for every 100 µL of stock thiol-functionalized probes added. Hybridization was performed by heating the oligonucleotide mixtures in an oil bath at 94ºC for 2 minutes and then allowed to slowly cool in oil bath to room temperature for 3 hours.

Following the hybridization, 20 µL of gold-coated magnetic particles (1 mg/mL) were added to a microcentrifuge tube and magnetically decanted. The oligonucleotide mixtures were then added to the particles (100 µL) and the tubes were placed on a rotating mixer for 24 hours. The particles were washed in 20 µL of TE buffer (10 mM NaCl, 10 mM Tris, 1 mM EDTA, 0.1% Tween 20).

Hybridization detection

Particles were added to 1 mM MCH with 0.1% Tween 20 and left for 24 hours on a rotating mixer. Particles were then magnetically decanted and washed three times in TE buffer.

To bind the oligonucleotides, 50 µL of particles were magnetically decanted and 100 µL of Millipore water with 0.1% Tween 20 and 52.5 µl of the above oligonucleotide solution were added. The microcentrifuge tubes were covered with aluminum foil and placed on a rotating mixer for 2 hours. Samples were magnetically decanted and washed three times in Millipore water with 0.1% Tween 20.

Hybridization was performed by diluting the complementary or non-complementary oligonucleotides to 5 µM in PBS buffer (0.3 M, pH 7) with 3% dextran sulfate and adding 20 µL to 20 µL of particles (1 mg/mL) following magnetic decantation. Particles were placed in a 94ºC oil bath for 3 minutes, then placed on a rotating mixer in an oven held at 45ºC for 4 hours, then cooled to room

temperature and left for 12 hours. Particles were washed three times in TE buffer and resuspended in the same.

Raman spectroscopy

A 20 µL drop of particles was placed on a glass slide with a hydrophobic coating. Raman scattering spectra of the particles were recorded in the 160-2400 cm^{-1} range on a Raman spectrometer (Tornado Spectral Systems) equipped with a near-IR laser diode (785 nm). The laser output power was 100 mW. For each spectrum, 15 acquisitions of 20 seconds each were recorded. Spectra were normalized using peak heights associated with the alkane chain linkers.

Results and Discussion

Particle synthesis

We grew gold spikes on silica-coated iron oxide spheres using a two-step method; first, CTAB-stabilized gold seeds were bound to the silica surface, then the seeds were grown into spiky particles using an aqueous, CTAB-based growth solution (Figure 1). To bind gold seeds to the surface, the silica-coated magnetic particles were functionalized with thiol groups (11-mercaptoundecanoic acid, MUA) that extended from the amine-functionalized surface (3-aminopropyltriethoxysilane, APTES), forming a mixed amine/thiol layer, as shown in previous work.[46] TEM images showed that gold seed binding occurred on the particles (Figure 2a-b). When the seeded particles were placed in the growth solution, the seeds grew into anisotropic shells (Figure 2c-d).

Figure 2: TEM images of a-b) silica-functionalized magnetite particles with gold seeds bound to surface and c-d) gold-shells grown on particles

For all steps in the synthesis, magnetic separation was used to wash the particles. During these steps, the particles were easily dispersed in solution and quickly separated out under the influence of a magnet. A SQUID magnetometer was used to obtain magnetization curves of the particles before and after gold coating (Figure 3). The saturation magnetization (M_s) of the silica-coated iron oxide particles was 32 emu/g and after gold shell coating, it was 9 emu/g. The silica-iron oxide core of the particles makes up 40-50% of the weight of the particles (estimated using the TEM-determined particle sizes) giving an adjusted saturation magnetization of 18-23 emu/g, which when compared with the measured 32 emu/g before gold shell coating suggests that some reduction in magnetization occurs upon coating. Others have also observed a reduction in particle magnetization upon coating.[47,48] Despite this reduction, particle separation times were still fast (less than two minutes).

Figure 3: Magnetization curves of silica-coated iron oxide particles before (solid) and after (dashed) gold/silver shell coating. The inset shows the small amount of hysteresis occurring at low magnetic fields

The low remanent magnetization (less than 1 emu/g, Figure 3 inset) suggests that the particles are not completely superparamagnetic, but experimental observations along with theoretical calculations lead to the conclusion that the particles behave superparamagnetically in practical applications.

SERS measurement of oligonucleotide probes

The signal enhancement of SERS is a highly distance-dependent phenomenon.[31,49-53] To determine which future applications of the particles would be possible or ideal, it is important to characterize the distance dependence specific to the particles. Other researchers have used oligonucleotide “rulers” to characterize the distance-dependence enhancement;[49,50,53] as the actual

relationship between enhancement and distance from the surface will vary with different substrates,[51] oligonucleotide rulers were used to characterize the relationship for the spiky particle surfaces. We bound seven different thiolated oligonucleotides to the particles, each featuring three adenine bases at different positions within a series of cytosine bases (Table 1i-vii), as well as an all cytosine oligonucleotide for a baseline (Table 1viii).

The Raman spectra following oligonucleotide binding are shown in Figure 4. Spectra were normalized using the peak at 1035 cm^{-1}, which corresponds to a C-C stretching absorption (mostly due to the alkane spacer) and varies little between oligonucleotide sequences. Normalization was used because of bound concentration variations with oligonucleotide type. Two replicates were prepared for each oligonucleotide type and are shown overlaid; generally, there was high reproducibility between samples. The relative peak heights associated with adenine bases and cytosine bases vary with adenine position. Specifically, peaks that increase with the proximity of adenine to the surface are at 748 cm^{-1}, 1338 cm^{-1}, and 1472 cm^{-1}; peaks that increase with the proximity of cytosine to the surface are at 764 cm^{-1}, 1300 cm^{-1}, and 1645 cm^{-1}. Previous research has shown that non-thiolated oligonucleotides adsorbed non-specifically to SERS substrates have signals that vary significantly with adenine/cytosine content but do not vary significantly when adenine position is changed;[54] we thus conclude that the oligonucleotides are most likely, on average, oriented in a stretched, upright or slightly angled position with the sulfur group bound to the gold surface. Previous research also confirms that this is the most likely result.[31,50,55]

Table 1: Oligonucleotide sequences used as "rulers"

	Position of AAA	Oligonucleotide Sequence
i	1	5'-CCCCCCCCCCCCAAA-3'-$(CH_3)_3$-S-
ii	2	5'-CCCCCCCCCCCAAAC-3'-$(CH_3)_3$-S-
iii	4	5'-CCCCCCCCCAAACCC-3'-$(CH_3)_3$-S-
iv	5	5'-CCCCCCCCAAACCCC-3'-$(CH_3)_3$-S-
v	7	5'-CCCCCCAAACCCCCC-3'-$(CH_3)_3$-S-

vi	10	5’-CCCAAACCCCCCCCC-3’-$(CH_3)_3$-S-
vii	13	5’-AAACCCCCCCCCCCC-3’-$(CH_3)_3$-S-
viii	-	5’-CCCCCCCCCCCCCCC-3’-$(CH_3)_3$-S-

Figure 4: SERS spectra of oligonucleotide “rulers” bound to spiky gold-coated particles. The rulers (i-vii) correspond to those listed in Table 1. Two spectra are shown overlaid for each oligonucleotide.

We fit the normalized intensity of the peak at 1338 cm^{-1} (adenosine ring stretching)[56] to a theoretical model that others have used to describe distance dependence,[50-53]

$$I = \left(1 + \frac{x}{a}\right)^{-10}$$

where x is the distance from the surface and a is the average radius of curvature of the SERS active structures. The model assumes a surface of electromagnetically isolated ellipsoidal protrusions of equal radius of curvature, *a*; since few real substrates fit this ideal model, the true distance dependence may not be x^{-10}, but this value is used for comparison with other work.

The length of the oligonucleotides includes the spacer group, bound to gold through the sulfur atom, and the chain of fifteen bases. The approximate length of the spacer group bound to gold is 0.83 nm.[57] We use 0.7 nm as an upper-limit of the length per base of the single stranded oligonucleotides.[58,59] Again, as an upper-limit, we assume that the oligonucleotides are oriented normal to the surface. Thus, we estimate a maximum distance between each base and the gold surface, x, to be $0.83 + 0.7n$, where n is the position of the base in the chain.

The data was fit to the model by summing the calculated intensities of the three adenine bases and fitting it to the experimental intensities using a nonlinear least-squares fit. The solid red line in Figure 5 shows the values obtained by the model. The theoretical radius of curvature, *a*, was 23 nm, a value which is in the range of

the substrate features observed by TEM if the theoretical model is taken to be suitable for the substrate.

Figure 5: Raman peak intensity (I_{1338}) after normalization using the peak intensity at 1035 cm^{-1} for oligonucleotides with different adenine group positions. The red line shows a fit to the data based on the distance dependence of the SERS signal. Error bars indicate a 95% confidence interval.

Investigating signal differences between ssDNA and dsDNA

Detecting DNA hybridization on the particles presents a challenge. Ideally, a label-free method would be used, where a change in signal occurs directly upon target binding to the probe. The above results, along with those seen in literature,[28-33] show that the Raman signal can vary with base composition, so it might be expected that DNA hybridization would present a different signal.

An alternative route to detect DNA hybridization that still does not require an extrinsic tag is to use a hairpin probe with a Raman tag attached to the end (Figure 6). This method takes advantage of the distance dependence of the SERS signal. Before adding a hybridizing target, the probe forms a hairpin structure that draws the Raman tag to the surface, so the signal from the Raman tag is high (closed position). When a target strand hybridizes with the probe, the hairpin will extend and bring the Raman tag away from the surface, so the signal from the Raman tag will decrease due to the distance dependence of the SERS enhancement (open position).

Figure 6: Scheme of hairpin probe with Raman tag, before and after hybridization to target strand

To test these two methods, we first tried performing the hybridization steps in solution using the thiolated probe DNA combined with complementary or non-

complementary DNA, or without any additional DNA (binding probe ssDNA to the surface). Assuming that the complementary DNA fully hybridizes with the probe DNA, this gives a potential maximum signal change while avoiding the challenge of performing hybridization to a surface-bound probe.

The signals from the case of label-free, direct detection (where no Raman tag was used) are shown in

Figure 7a. Spectra were normalized using the intensity at 1087 cm^{-1}, which corresponds to the C6 alkane chain linker. No obvious changes could be observed between the case where dsDNA should have been binding compared with the case where ssDNA should have been binding.

We performed a similar experiment with the thiolated hairpin probe, using Cy5 as a Raman tag. In this case, the signal from the Cy5 tag should be lower in the case of dsDNA binding (probe and complementary oligonucleotides) compared with ssDNA binding. Figure 7a demonstrates that this is what is observed. Spectra were normalized using the intensity at 1023 cm^{-1}, which corresponds to the C3 alkane chain linker. We observe similar peak intensities from the thiolated three carbon alkane chain linker (C-S bonds at 707 and 646 cm^{-1} and alkane chain at 1023 cm^{-1}), but lower peak intensities (50-60% of that from ssDNA only) from the Cy5 tag (558 cm^{-1}, many peaks in region from 1100-1600 cm^{-1} including 1189, 1363, and 1600 cm^{-1}).

Figure 7: Normalized SERS spectra a) without and b) with a Cy5 tag of i) oligonucleotide probes only and ii) oligonucleotide probes hybridized with complementary oligonucleotides

Based on these results, the method using a hairpin probe with a Raman tag seemed more promising as it resulted in a larger signal change between ssDNA and dsDNA and validates the efficiency of the spiky gold shell nanoparticles as SERS transducer.

Hybridization detection

The above results demonstrated that the signal changes when double-stranded versus single-stranded oligonucleotides are bound to the surface (Figure 7b). A next step is to detect hybridization between target DNA and probe DNA bound to the surface. We bound the Cy5-tagged hairpin probe to the MCH functionalized surface of the particles using an insertion method[60], then compared the signal from hybridization with 5 μM of complementary and non-complementary targets to the probes. The high concentration of target oligonucleotides WAS used to ensure that binding was favoured in the equilibrium.

The obtained Raman signal from these samples was normalized using the intensity of the peak at 1087 cm^{-1} (corresponding to the six carbon alkane linker, thus normalizing based on the amount of probe DNA bound to the surface). The signal of Cy5 is lower when complementary DNA is used compared with non-complementary DNA, which is consistent with hybridization causing the hairpin probe to open and increase the distance of Cy5 from the surface (Figure 8). In Figure 8b, the difference is highlighted by the fact that the peak at 712 cm^{-1}, corresponding to the C-S bond of the thiol linker, is of similar intensity for all samples, while the peaks corresponding to Cy5 (558, 1189, 160 cm^{-1}) for the sample using complementary DNA are 60-70% of the intensity of peaks from the probe only or the sample using non-complementary DNA.

Figure 8: a) Normalized SERS spectra and b) average peak height of i) Cy5-tagged oligonucleotide hairpin probes, ii) hybridization with complementary oligonucleotides and iii) hybridization with non-complementary oligonucleotides. Error bars indicate 95% confidence intervals.

Conclusion

We synthesized nanostructured gold-coated magnetic particles and demonstrated their use as tools for oligonucleotide separation and SERS detection. The particles are magnetically separable, exhibiting superparamagnetic behavior. The distance dependence of the signal was harnessed to detect oligonucleotide hybridization using a hairpin probe with a Raman tag.

This result is the first example, to our knowledge, of using nanostructured gold-coated magnetic particles to directly detect oligonucleotide hybridization using SERS. The method does not require the use of an extrinsic tag or a secondary hybridization step. It may be possible to extend the concept to detect other biomolecules using different probes that change conformation upon biomolecule binding, such as certain aptamers. The work presented here gives the first steps towards an advanced assay for biomolecule detection and/or separation. A next step could involve using the particles in a microfluidic set-up, where additional control and separation is made possible using magnetic forces.

Acknowledgements

This work was supported by the Natural Sciences and Engineering Research Council of Canada (NSERC) and the Erasmus-sponsored International Doctoral School in Functional Materials (IDS-FunMat).

References

[1] S.O. Kelley, C.A. Mirkin, D.R. Walt, R.F. Ismagilov, M. Toner, E.H. Sargent, Advancing the speed, sensitivity and accuracy of biomolecular detection using multi-length-scale engineering, Nature Nanotechnology. 9 (2014) 969–980. doi:10.1038/nnano.2014.261.

[2] N.L. Rosi, C.A. Mirkin, Nanostructures in Biodiagnostics, Chem. Rev. 105 (2005) 1547–1562. doi:10.1021/cr030067f.

[3] B. Rittich, A. Španová, SPE and purification of DNA using magnetic particles, Journal of Separation Science. 36 (2013) 2472–2485.

doi:10.1002/jssc.201300331.
[4] K. Niemirowicz, K.H. Markiewicz, A.Z. Wilczewska, H. Car, Magnetic nanoparticles as new diagnostic tools in medicine, Advances in Medical Sciences. 57 (2012) 196–207. doi:10.2478/v10039-012-0031-9.
[5] M. Shinkai, Functional magnetic particles for medical application, Journal of Bioscience and Bioengineering. 94 (2002) 606–613. doi:10.1016/S1389-1723(02)80202-X.
[6] E. Paleček, M. Fojta, Magnetic beads as versatile tools for electrochemical DNA and protein biosensing, Talanta. 74 (2007) 276–290. doi:10.1016/j.talanta.2007.08.020.
[7] J. Wang, A.-N. Kawde, A. Erdem, M. Salazar, Magnetic bead-based label-free electrochemical detection of DNA hybridization, Analyst. 126 (2001) 2020–2024. doi:10.1039/B106343J.
[8] O. Olsvik, T. Popovic, E. Skjerve, K.S. Cudjoe, E. Hornes, J. Ugelstad, et al., Magnetic separation techniques in diagnostic microbiology, Clin. Microbiol. Rev. 7 (1994) 43–54. doi:10.1128/CMR.7.1.43.
[9] G. De Las Cuevas, J. Faraudo, J. Camacho, Low-Gradient Magnetophoresis through Field-Induced Reversible Aggregation, J. Phys. Chem. C. 112 (2008) 945–950. doi:10.1021/jp0755286.
[10] J. Lim, S.A. Majetich, Composite magnetic–plasmonic nanoparticles for biomedicine: Manipulation and imaging, Nano Today. 8 (2013) 98–113. doi:10.1016/j.nantod.2012.12.010.
[11] M. Benelmekki, C. Caparros, A. Montras, R. Gon ßalves, S. Lanceros-Mendez, L.M. Martinez, Horizontal low gradient magnetophoresis behaviour of iron oxide nanoclusters at the different steps of the synthesis route, J. Nanopart. Res. 13 (2011) 3199–3206. doi:10.1007/s11051-010-0218-6.
[12] Y. Lee, J. Lee, C.J. Bae, J.G. Park, H.J. Noh, J.H. Park, et al., Large-Scale Synthesis of Uniform and Crystalline Magnetite Nanoparticles Using Reverse Micelles as Nanoreactors under Reflux Conditions, Adv. Funct. Mater. 15 (2005) 503–509. doi:10.1002/adfm.200400187.
[13] D. Cialla, A. März, R. Böhme, F. Theil, K. Weber, M. Schmitt, et al., Surface-enhanced Raman spectroscopy (SERS): progress and trends, Anal. Bioanal. Chem. 403 (2012) 27–54.
[14] E.E. Bedford, S. Boujday, C.M. Pradier, F.X. Gu, Nanostructured and spiky gold in biomolecule detection: improving binding efficiencies and enhancing optical signals, RSC Adv. 5 (2015) 16461–16475. doi:10.1039/C4RA13544J.
[15] Q. Wei, H.-M. Song, A.P. Leonov, J.A. Hale, D. Oh, Q.K. Ong, et al., Gyromagnetic imaging: dynamic optical contrast using gold nanostars with magnetic cores, J. Am. Chem. Soc. 131 (2009) 9728–9734.
[16] H.-M. Song, Q. Wei, Q.K. Ong, A. Wei, Plasmon-Resonant Nanoparticles and Nanostars with Magnetic Cores: Synthesis and Magnetomotive Imaging, ACS Nano. 4 (2010) 5163–5173. doi:10.1021/nn101202h.
[17] X. Miao, T. Wang, F. Chai, X. Zhang, C. Wang, W. Sun, A facile synthetic route for the preparation of gold nanostars with magnetic cores and their reusable

nanohybrid catalytic properties, Nanoscale. 3 (2011) 1189. doi:10.1039/c0nr00704h.
[18] P. Quaresma, I. Osório, G. Dória, P.A. Carvalho, A. Pereira, J. Langer, et al., Star-shaped magnetite@gold nanoparticles for protein magnetic separation and SERS detection, RSC Adv. 4 (2013) 3659. doi:10.1039/c3ra46762g.
[19] H. Zhou, J.-P. Kim, J.H. Bahng, N.A. Kotov, J. Lee, Self-Assembly Mechanism of Spiky Magnetoplasmonic Supraparticles, Adv. Funct. Mater. 24 (2013) 1439–1448. doi:10.1002/adfm.201302405.
[20] J. Li, J. Wu, X. Zhang, Y. Liu, D. Zhou, H. Sun, et al., Controllable Synthesis of Stable Urchin-like Gold Nanoparticles Using Hydroquinone to Tune the Reactivity of Gold Chloride, J. Phys. Chem. C. 115 (2011) 3630–3637. doi:10.1021/jp1119074.
[21] B.L. Sanchez-Gaytan, S.-J. Park, Spiky Gold Nanoshells, Langmuir. 26 (2010) 19170–19174. doi:10.1021/la1038969.
[22] B.L. Sanchez-Gaytan, P. Swanglap, T.J. Lamkin, R.J. Hickey, Z. Fakhraai, S. Link, et al., Spiky Gold Nanoshells: Synthesis and Enhanced Scattering Properties, J. Phys. Chem. C. 116 (2012) 10318–10324. doi:10.1021/jp300009b.
[23] N. Pazos-Pérez, S. Barbosa, L. Rodríguez-Lorenzo, P. Aldeanueva-Potel, J. Pérez-Juste, I. Pastoriza-Santos, et al., Growth of Sharp Tips on Gold Nanowires Leads to Increased Surface-Enhanced Raman Scattering Activity, J. Phys. Chem. Lett. 1 (2010) 24–27. doi:10.1021/jz900004h.
[24] P. Aldeanueva-Potel, E. Carbó-Argibay, N. Pazos-Pérez, S. Barbosa, I. Pastoriza-Santos, R.A. Alvarez-Puebla, et al., Spiked Gold Beads as Substrates for Single-Particle SERS, ChemPhysChem. 13 (2012) 2561–2565. doi:10.1002/cphc.201101014.
[25] S. Pedireddy, A. Li, M. Bosman, I.Y. Phang, S. Li, X.Y. Ling, Synthesis of Spiky Ag–Au Octahedral Nanoparticles and Their Tunable Optical Properties, J. Phys. Chem. C. 117 (2013) 16640–16649. doi:10.1021/jp4063077.
[26] I. Pastoriza-Santos, L.M. Liz-Marzán, N, N-Dimethylformamide as a Reaction Medium for Metal Nanoparticle Synthesis, Adv. Funct. Mater. 19 (2009) 679–688. doi:10.1002/adfm.200801566.
[27] H. Yuan, W. Ma, C. Chen, J. Zhao, J. Liu, H. Zhu, et al., Shape and SPR Evolution of Thorny Gold Nanoparticles Promoted by Silver Ions, Chem. Mater. 19 (2007) 1592–1600. doi:10.1021/cm062046i.
[28] E. Prado, N. Daugey, S. Plumet, L. Servant, S. Lecomte, Quantitative label-free RNA detection using surface-enhanced Raman spectroscopy, Chem. Commun. 47 (2011) 7425–7427. doi:10.1039/C1CC11925G.
[29] L. Guerrini, Ž. Krpetić, D. van Lierop, R.A. Alvarez-Puebla, D. Graham, Direct Surface-Enhanced Raman Scattering Analysis of DNA Duplexes, Angewandte Chemie. 127 (2015) 1160–1164. doi:10.1002/ange.201408558.
[30] E. Papadopoulou, S.E.J. Bell, Label-Free Detection of Single-Base Mismatches in DNA by Surface-Enhanced Raman Spectroscopy, Angew. Chem. Int. Ed. 50 (2011) 9058–9061. doi:10.1002/anie.201102776.
[31] A. Barhoumi, D. Zhang, F. Tam, Surface-enhanced Raman spectroscopy of DNA,

J. Am. Chem. Soc. (2008).
[32] J.L. Abell, J.M. Garren, J.D. Driskell, R.A. Tripp, Y. Zhao, Label-Free Detection of Micro-RNA Hybridization Using Surface-Enhanced Raman Spectroscopy and Least-Squares Analysis, J. Am. Chem. Soc. 134 (2012) 12889–12892. doi:10.1021/ja3043432.
[33] A. Barhoumi, N.J. Halas, Label-free detection of DNA hybridization using surface enhanced Raman spectroscopy, J. Am. Chem. Soc. 132 (2010) 12792–12793.
[34] E. Papadopoulou, S.E.J. Bell, DNA reorientation on Au nanoparticles: label-free detection of hybridization by surface enhanced Raman spectroscopy, Chem. Commun. 47 (2011) 10966–10968. doi:10.1039/C1CC13705K.
[35] H.T. Ngo, H.-N. Wang, A.M. Fales, T. Vo-Dinh, Label-Free DNA Biosensor Based on SERS Molecular Sentinel on Nanowave Chip, Anal. Chem. 85 (2013) 6378–6383. doi:10.1021/ac400763c.
[36] H.T. Ngo, H.-N. Wang, T. Burke, G.S. Ginsburg, T. Vo-Dinh, Multiplex detection of disease biomarkers using SERS molecular sentinel-on-chip, Anal. Bioanal. Chem. 406 (2014) 3335–3344. doi:10.1007/s00216-014-7648-4.
[37] H.T. Ngo, H.-N. Wang, A.M. Fales, T. Vo-Dinh, Plasmonic SERS biosensing nanochips for DNA detection, Anal. Bioanal. Chem. 408 (2015) 1773–1781. doi:10.1007/s00216-015-9121-4.
[38] M.B. Wabuyele, T. Vo-Dinh, Detection of Human Immunodeficiency Virus Type 1 DNA Sequence Using Plasmonics Nanoprobes, Anal. Chem. 77 (2005) 7810–7815. doi:10.1021/ac0514671.
[39] H. Wang, X. Jiang, X. Wang, X. Wei, Y. Zhu, Bin Sun, et al., Hairpin DNA-Assisted Silicon/Silver-Based Surface-Enhanced Raman Scattering Sensing Platform for Ultrahighly Sensitive and Specific Discrimination of Deafness Mutations in a Real System, Anal. Chem. 86 (2014) 7368–7376. doi:10.1021/ac501675d.
[40] J. Chen, J. Jiang, X. Gao, G. Liu, G. Shen, R. Yu, A New Aptameric Biosensor for Cocaine Based on Surface-Enhanced Raman Scattering Spectroscopy, Chemistry - a European Journal. 14 (2008) 8374–8382. doi:10.1002/chem.200701307.
[41] K. Faulds, W.E. Smith, D. Graham, Evaluation of Surface-Enhanced Resonance Raman Scattering for Quantitative DNA Analysis, Anal. Chem. 76 (2003) 412–417. doi:10.1021/ac035060c.
[42] K. Faulds, F. McKenzie, W.E. Smith, D. Graham, Quantitative Simultaneous Multianalyte Detection of DNA by Dual-Wavelength Surface-Enhanced Resonance Raman Scattering, Angewandte Chemie. 119 (2007) 1861–1863.
[43] T. Leshuk, P. Everett, H. Krishnakumar, K. Wong, S. Linley, F. Gu, Mesoporous Magnetically Recyclable Photocatalysts for Water Treatment, J. Nanosci. Nanotechnol. 13 (2013) 3127–3132. doi:10.1166/jnn.2013.7396.
[44] W. Cheng, K. Tang, Y. Qi, J. Sheng, Z. Liu, One-step synthesis of superparamagnetic monodisperse porous Fe 3 O 4 hollow and core-shell spheres, Journal of Materials Chemistry. 20 (2010) 1799. doi:10.1039/b919164j.
[45] L. Wang, J. Li, Q. Jiang, L. Zhao, Water-soluble Fe3O4 nanoparticles with high solubility for removal of heavy-metal ions from waste water, Dalton Trans. 41 (2012) 4544–4551. doi:10.1039/C2DT11827K.

[46] M. Ben Haddada, J. Blanchard, S. Casale, J.-M. Krafft, A. Vallée, C. Méthivier, et al., Optimizing the immobilization of gold nanoparticles on functionalized silicon surfaces: amine- vs thiol-terminated silane, Gold Bull. 46 (2013) 335–341. doi:10.1007/s13404-013-0120-y.

[47] A.-H. Lu, E.L. Salabas, F. Schüth, Magnetic nanoparticles: synthesis, protection, functionalization, and application, Angew. Chem. Int. Ed. 46 (2007) 1222–1244. doi:10.1002/anie.200602866.

[48] A.P. Philipse, M. Van Bruggen, C. Pathmamanoharan, Magnetic silica dispersions: preparation and stability of surface-modified silica particles with a magnetic core, Langmuir. 10 (1994) 92–99. doi:10.1021/la00013a014.

[49] S. Lal, N.K. Grady, G.P. Goodrich, N.J. Halas, Profiling the Near Field of a Plasmonic Nanoparticle with Raman-Based Molecular Rulers, Nano Lett. 6 (2006) 2338–2343. doi:10.1021/nl061892p.

[50] N.E. Marotta, K.R. Beavers, L.A. Bottomley, Limitations of Surface Enhanced Raman Scattering in Sensing DNA Hybridization Demonstrated by Label-Free DNA Oligos as Molecular Rulers of Distance-Dependent Enhancement, Anal. Chem. 85 (2013) 1440–1446. doi:10.1021/ac302454j.

[51] C.A. Murray, Molecule-Silver Separation Dependence, in: Surface Enhanced Raman Scattering, Springer US, Boston, MA, 1982: pp. 203–221. doi:10.1007/978-1-4615-9257-0_11.

[52] B.J. Kennedy, S. Spaeth, M. Dickey, K.T. Carron, Determination of the Distance Dependence and Experimental Effects for Modified SERS Substrates Based on Self-Assembled Monolayers Formed Using Alkanethiols, J. Phys. Chem. B. 103 (1999) 3640–3646. doi:10.1021/jp984454i.

[53] F.M. Liu, P.A. Köllensperger, M. Green, A. Cass, A note on distance dependence in surface enhanced Raman spectroscopy, Chemical Physics Letters. 430 (2006) 173–176. doi:10.1016/j.cplett.2006.08.091.

[54] E. Papadopoulou, S.E.J. Bell, Label-Free Detection of Nanomolar Unmodified Single- and Double-Stranded DNA by Using Surface-Enhanced Raman Spectroscopy on Ag and Au Colloids, Chemistry - a European Journal. 18 (2012) 5394–5400. doi:10.1002/chem.201103520.

[55] W.J. Parak, T. Pellegrino, C.M. Micheel, D. Gerion, S.C. Williams, A.P. Alivisatos, Conformation of Oligonucleotides Attached to Gold Nanocrystals Probed by Gel Electrophoresis, Nano Lett. 3 (2002) 33–36. doi:10.1021/nl025888z.

[56] S.E.J. Bell, N.M.S. Sirimuthu, Surface-enhanced Raman spectroscopy (SERS) for sub-micromolar detection of DNA/RNA mononucleotides, J. Am. Chem. Soc. 128 (2006) 15580–15581. doi:10.1021/ja066263w.

[57] C.D. Bain, E.B. Troughton, Y.T. Tao, J. Evall, G.M. Whitesides, R.G. Nuzzo, Formation of monolayer films by the spontaneous assembly of organic thiols from solution onto gold, J. Am. Chem. Soc. 111 (1989) 321–335. doi:10.1021/ja00183a049.

[58] J.B. Mills, E. Vacano, P.J. Hagerman, Flexibility of single-stranded DNA: use of gapped duplex helices to determine the persistence lengths of Poly(dT) and Poly(dA), Journal of Molecular Biology. 285 (1999) 245–257.

doi:10.1006/jmbi.1998.2287.
[59] S.B. Smith, Y. Cui, C. Bustamante, Overstretching B-DNA: the elastic response of individual double-stranded and single-stranded DNA molecules, Science. 271 (1996) 795–799.
[60] E.A. Josephs, T. Ye, Nanoscale Spatial Distribution of Thiolated DNA on Model Nucleic Acid Sensor Surfaces, ACS Nano. 7 (2013) 3653–3660. doi:10.1021/nn400659m.

Figure Caption

Figure 1: Schematic diagram of spiky particle synthesis steps. Gold seeds are bound to a silica-coated magnetite particle, then grown into gold spikes using a gold salt and CTAB bath solution.

Figure 2: TEM images of a-b) silica-functionalized magnetite particles with gold seeds bound to surface and c-d) gold-shells grown on particles

Figure 3: Magnetization curves of silica-coated iron oxide particles before (solid) and after (dashed) gold/silver shell coating. The inset shows the small amount of hysteresis occurring at low magnetic fields

Figure 4: SERS spectra of oligonucleotide “rulers” bound to spiky gold-coated particles. The rulers (i-vii) correspond to those listed in Table 1. Two spectra are shown overlaid for each oligonucleotide.

Figure 5: Raman peak intensity (I1338) after normalization using the peak intensity at 1035 cm-1 for oligonucleotides with different adenine group positions. The red line shows a fit to the data based on the distance dependence of the SERS signal. Error bars indicate a 95% confidence interval.

Figure 6: Scheme of hairpin probe with Raman tag, before and after hybridization to target strand

Figure 7: Normalized SERS spectra a) without and b) with a Cy5 tag of i) oligonucleotide probes only and ii) oligonucleotide probes hybridized with complementary oligonucleotides

Figure 8: a) Normalized SERS spectra and b) average peak height of i) Cy5-tagged oligonucleotide hairpin probes, ii) hybridization with complementary oligonucleotides and iii) hybridization with non-complementary oligonucleotides. Error bars indicate 95% confidence intervals.

***Checklist**

Corresponding Author: Souhir Boujday

• E-mail address: souhir.boujday@upmc.fr

• Full postal address Sorbonne Universités, UPMC Univ Paris 06, CNRS, Laboratoire de Réactivité de Surface (LRS), UMR 7197, 4 Place Jussieu, Case 178, F-75252, Paris, France

All necessary files have been uploaded:

Manuscript done

• Include keywords done

• All figures (include relevant captions) done

• All tables (including titles, description, footnotes) done

• Ensure all figure and table citations in the text match the files provided done

• Graphical Abstracts / Highlights files (where applicable)

***List of Three Potential Reviewers**

Referee

Sabine Szunerits

sabine.szunerits@iri.univ-lille1.fr

Université des sciences et technologie de Lille - Lille 1

Wolfgang Knoll

Wolfgang.Knoll@ait.ac.at

Austrian Institute of Technology

Raju Vijayaraghavan Ramanujan

RAMANUJAN@NTU.EDU.SG

Nanyang Technological University

Jakub Dostalek

Jakub.Dostalek@ait.ac.at

Austrian Institute of Technology

Anne Vallee

anne.vallee@uvsq.fr

Institut Lavoisier – UVSQ

Figure1
Click here to download high resolution image

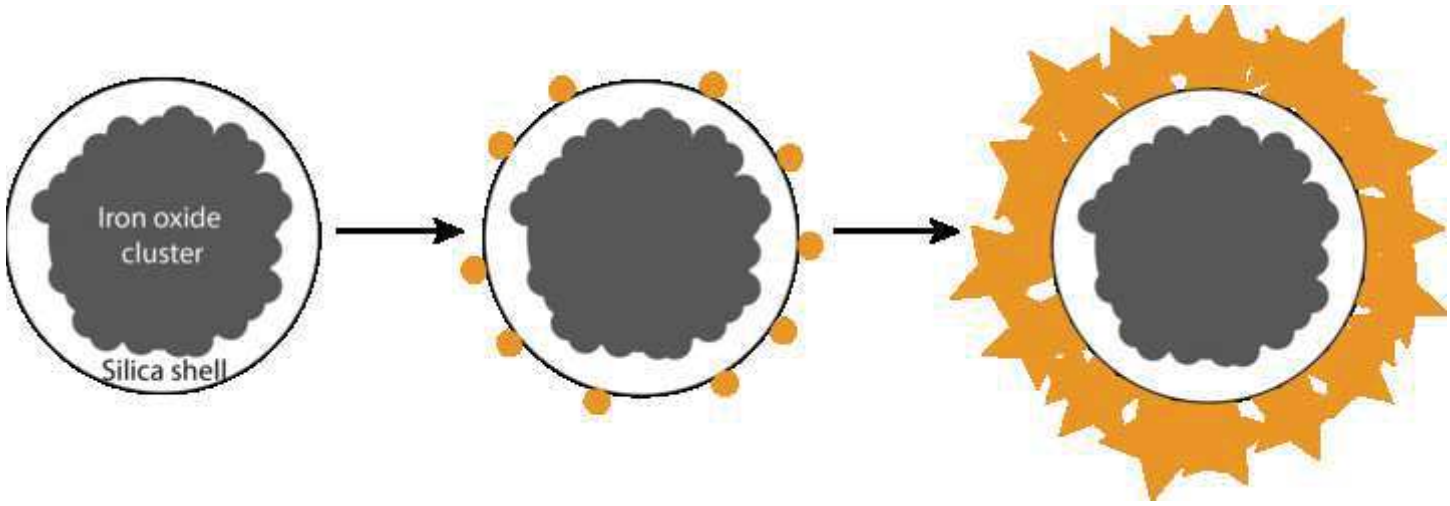

Figure2
Click here to download high resolution image

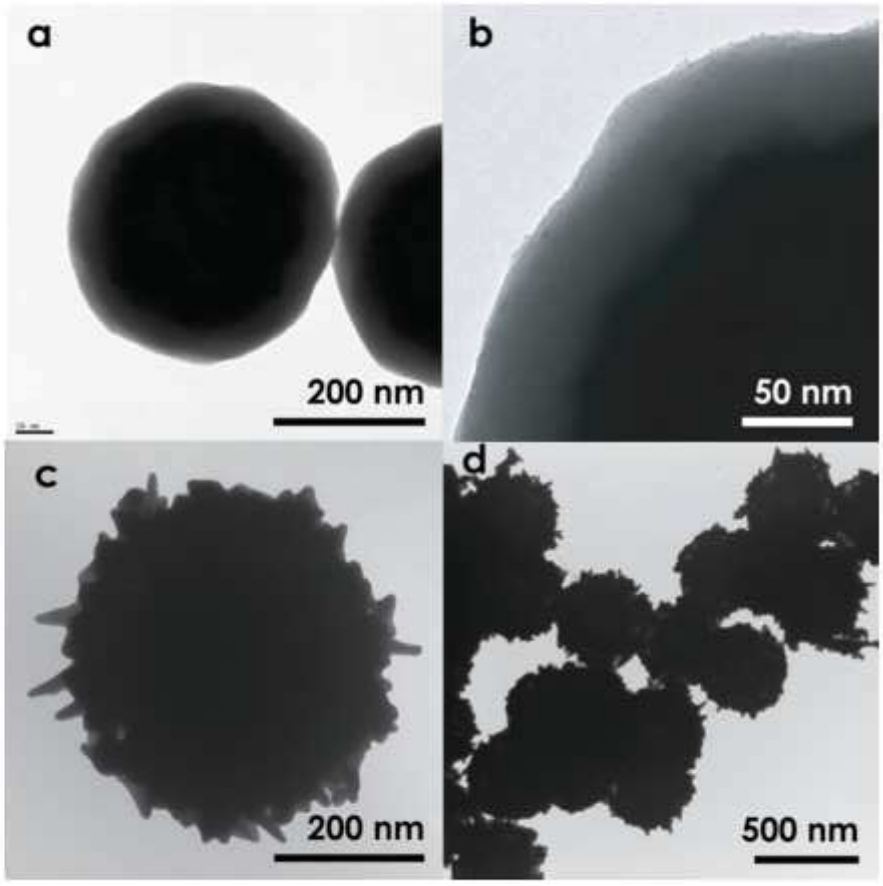

Figure3
Click here to download high resolution image

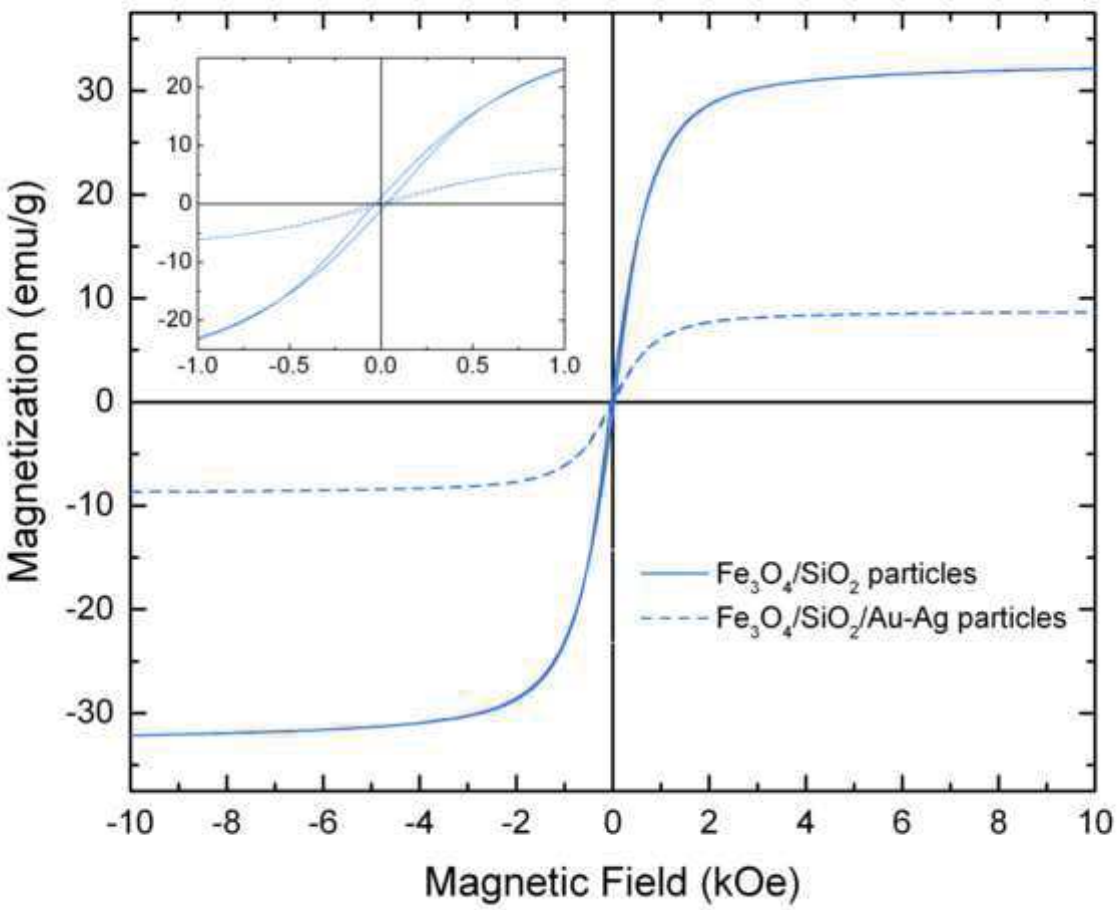

Figure4
Click here to download high resolution image

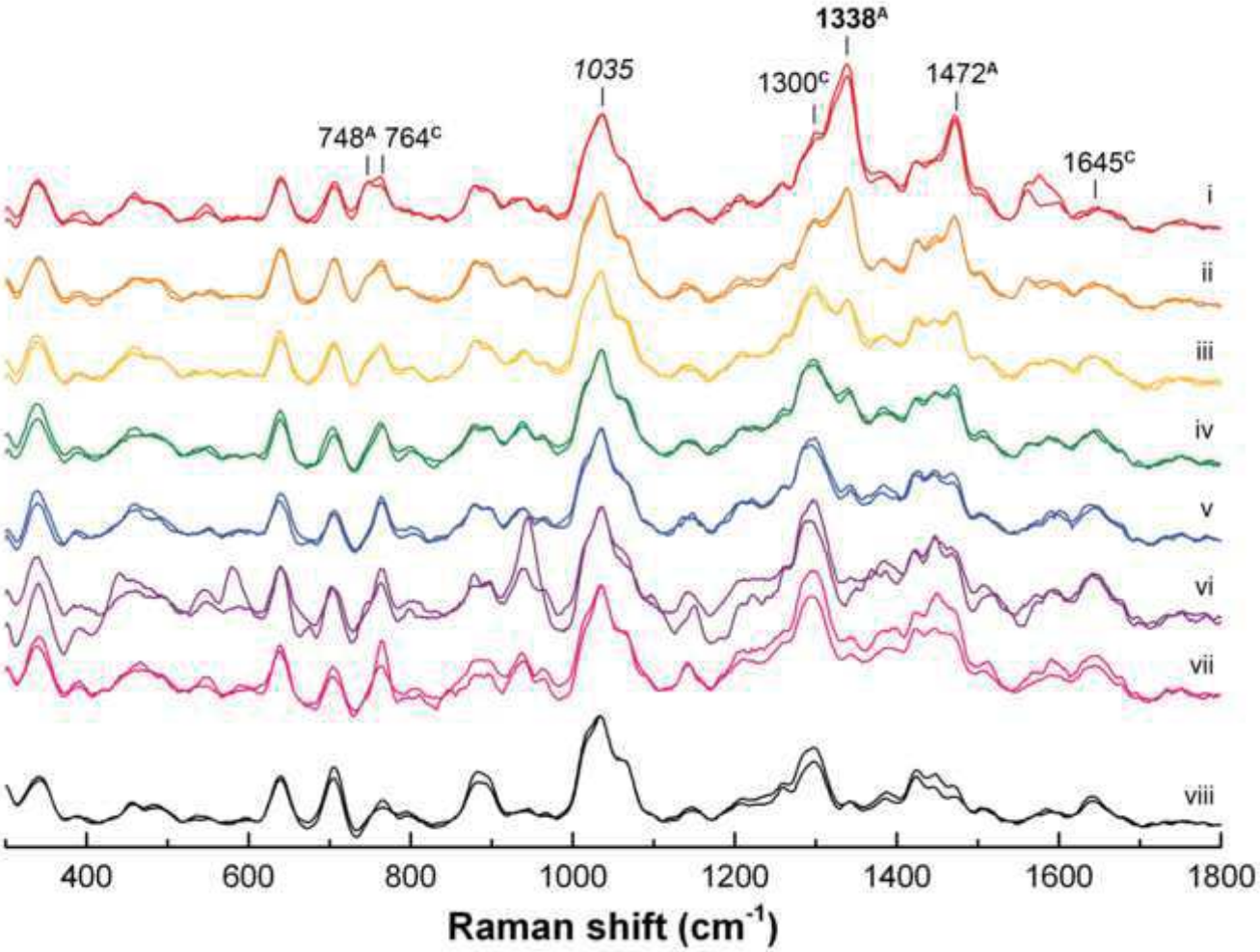

Figure5
Click here to download high resolution image

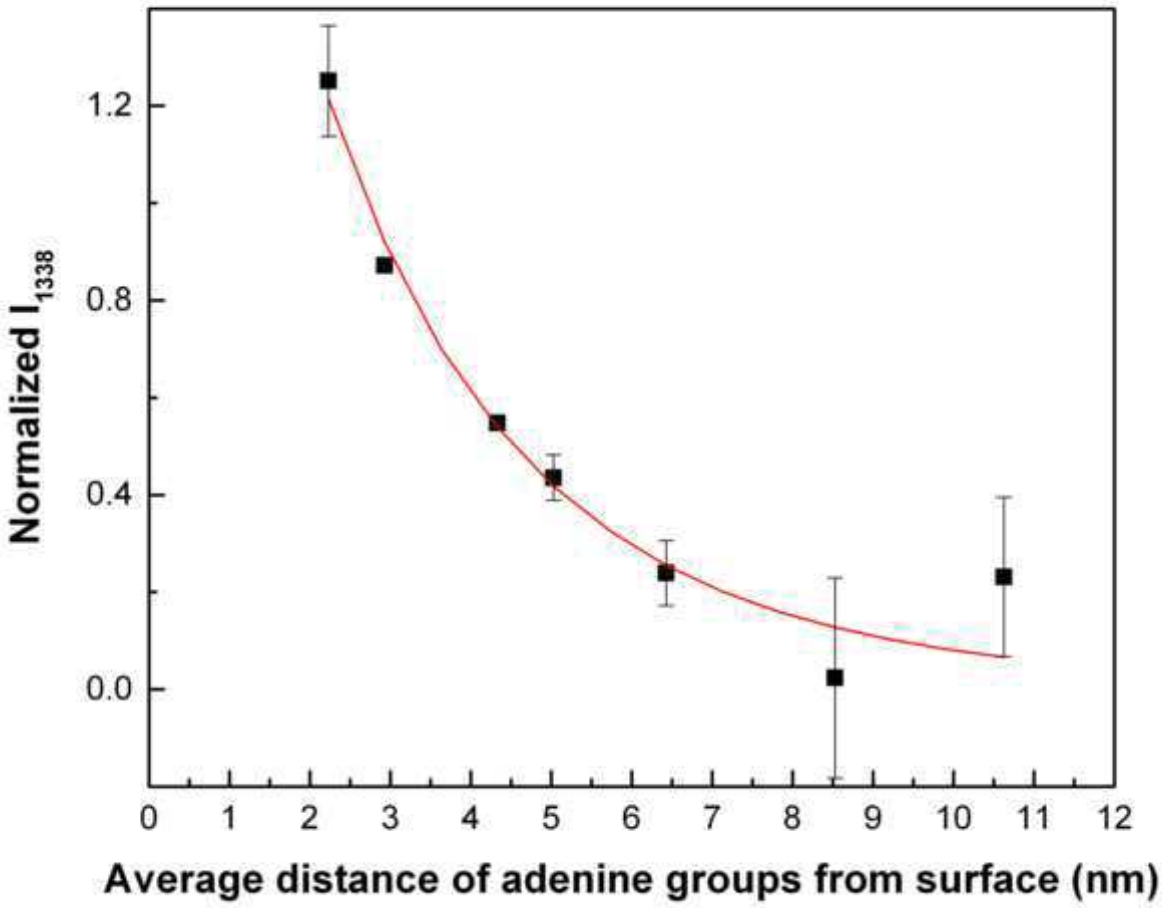

Figure6
Click here to download high resolution image

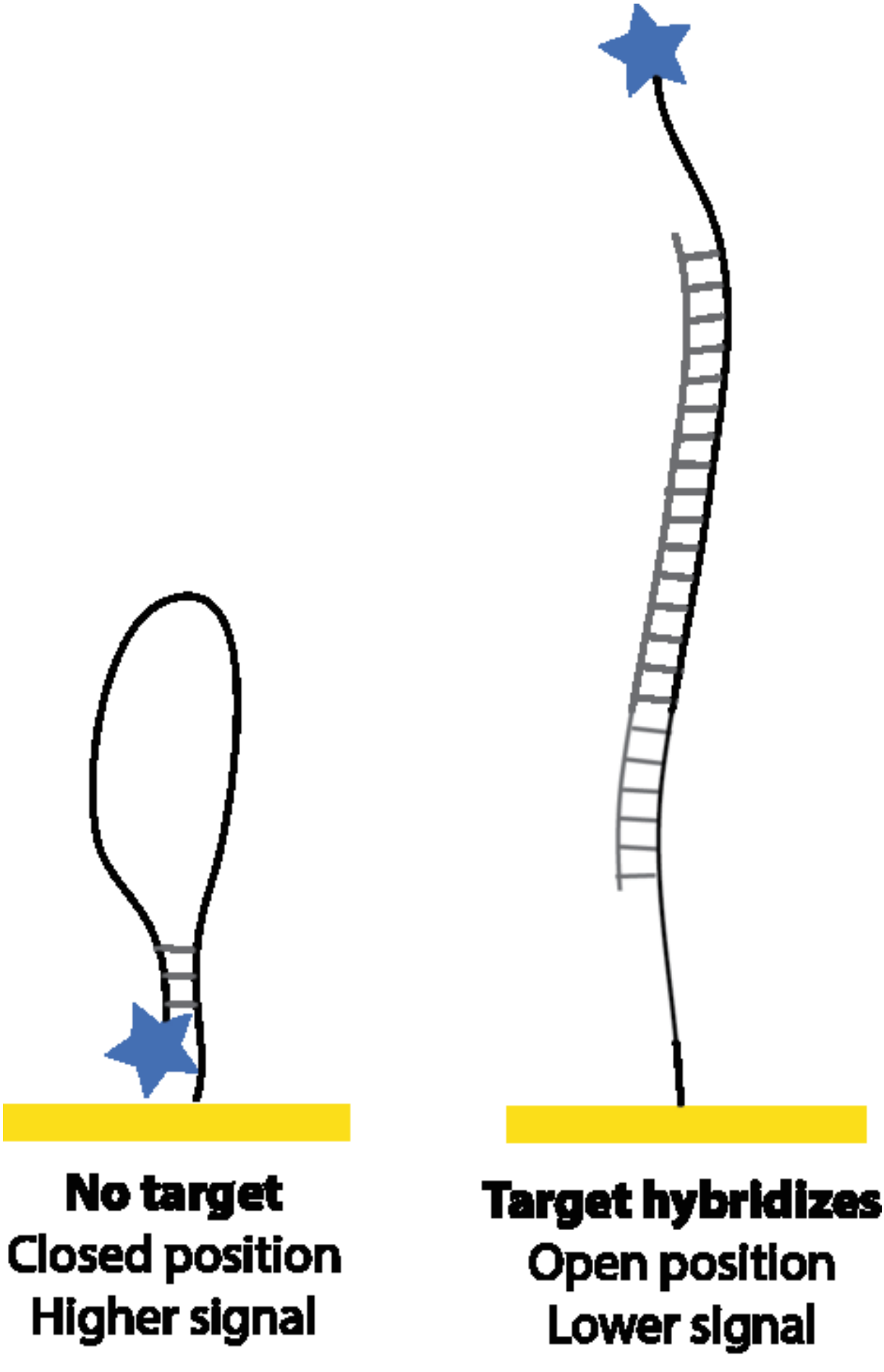

Figure7
Click here to download high resolution image

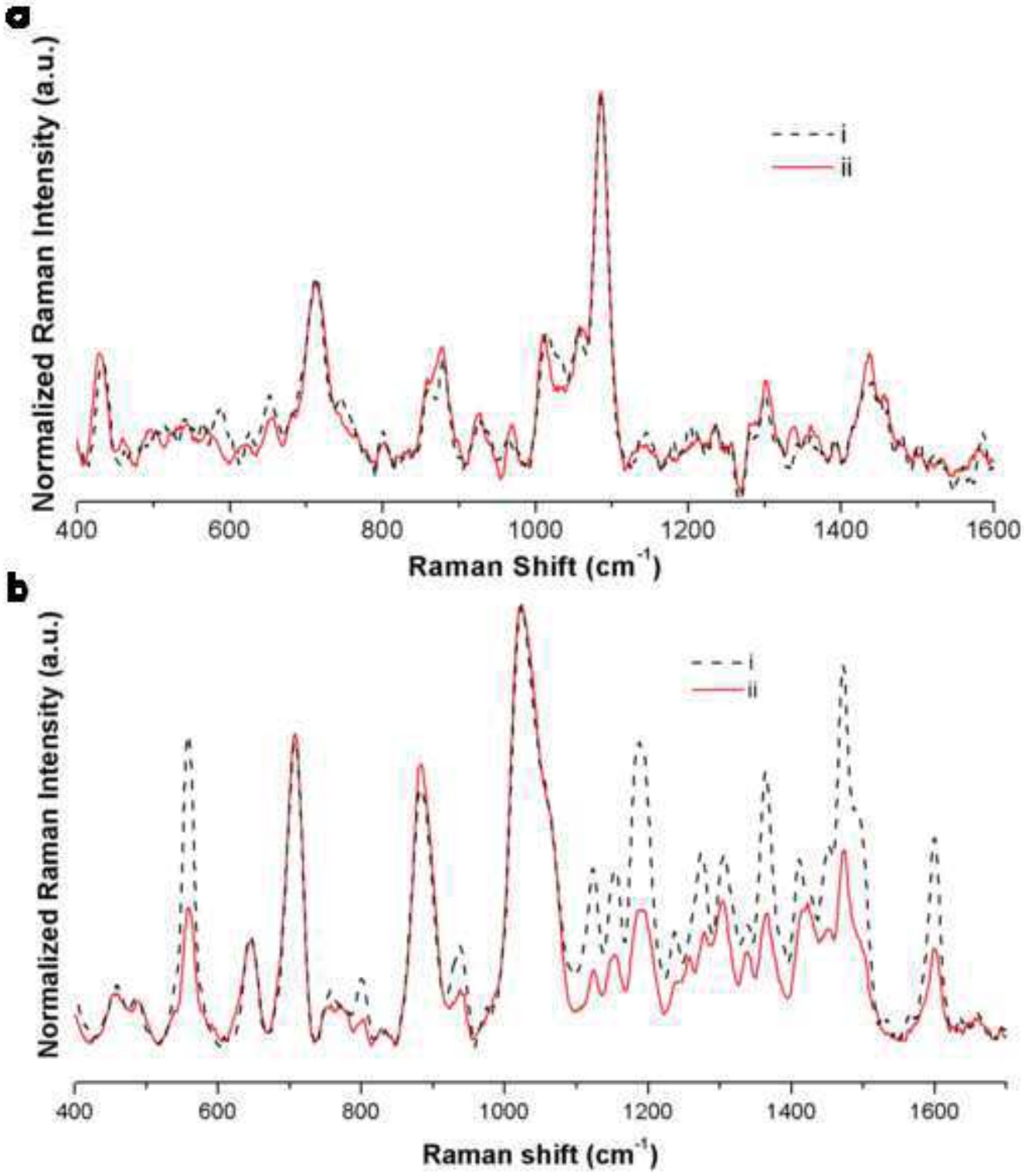

Figure8
Click here to download high resolution image